

Vesicoureteral Reflux Detection with Reliable Probabilistic Outputs

Harris Papadopoulos^a, George Anastassopoulos^b

^a*Frederick University, 7 Y. Frederickou St., Palouriotisa, Nicosia 1036, Cyprus*

^b*Medical Informatics Laboratory, Democritus University of Thrace, GR-68100, Alexandroupolis, Greece*

Abstract

Vesicoureteral Reflux (VUR) is a pediatric disorder in which urine flows backwards from the bladder to the upper urinary tract. Its detection is of great importance as it increases the risk of a Urinary Tract Infection, which can then lead to a kidney infection since bacteria may have direct access to the kidneys. Unfortunately the detection of VUR requires a rather painful medical examination, called voiding cysteourethrogram (VCUG), that exposes the child to radiation. In an effort to avoid the exposure to radiation required by VCUG some recent studies examined the use of machine learning techniques for the detection of VUR based on data that can be obtained without exposing the child to radiation. This work takes one step further by proposing an approach that provides lower and upper bounds for the conditional probability of a given child having VUR. The important property of these bounds is that they are guaranteed (up to statistical fluctuations) to contain well-calibrated probabilities with the only requirement that observations are independent and identically distributed (i.i.d.). Therefore they are much more informative and reliable than the plain yes/no answers provided by other techniques.

Keywords: Venn Prediction, Neural Networks, Probabilistic Classification, Multiprobability Prediction

Email addresses: h.papadopoulos@frederick.ac.cy (Harris Papadopoulos),
anasta@med.duth.gr (George Anastassopoulos)

1. Introduction

Vesicoureteral Reflux (VUR) is a pediatric disorder that has potentially very serious consequences as it might lead to a kidney infection (pyelonephritis). Specifically, in VUR urine flows abnormally from the bladder back into one or both ureters and, in some cases, into one or both kidneys. The severity of VUR is classified into five grades, grade I being the least severe and grade V being the most severe. The disorder increases the risk of Urinary Tract Infections (UTIs), which, if left untreated, can lead to kidney damage. Therefore young children diagnosed with UTI should be further examined for VUR. However, the principal medical examination for the detection of VUR, the *voiding cysteourethrogram* (VCUG), is not only a painful procedure, but also demands the exposure of the child to radiation. For this reason, the development of a technique that would help avoid VCUG and consequently the exposure to radiation is very desirable.

The use of machine learning techniques towards this goal using as inputs clinical and laboratorial information that can be obtained without the need of radiation exposure was examined in some recent studies [3, 8, 9, 10]. The techniques proposed in these studies however only provide a yes or no output, without giving any further information about how much one can rely on this output. This is of course a disadvantage of most existing medical decision support systems, as this is what most conventional machine learning techniques provide. Nevertheless it is a significant disadvantage, especially in a medical setting where some indication about the likelihood of each diagnosis is of paramount importance [5].

In this work we address this drawback with the use of a recently developed machine learning framework called *Venn Prediction* (VP). Venn Prediction was proposed in [18] while a detailed description of the framework can be found in [17]. It provides a way of extending conventional classifiers to develop techniques that produce *multiprobability predictions* without assuming anything more than i.i.d. observations. In effect multiprobability predictions are a set of probability distributions for the true classification of the new example, which can be summarized by lower and upper bounds for the conditional probability of each new example belonging to each one of the possible classes for the task in question. The resulting bounds are guaranteed to contain well-calibrated probabilities (up to statistical fluctuations).

Until now the VP framework has been combined with the k -Nearest Neighbour classifier in [17] and [2], with Support Vector Machines in [6, 19],

with Logistic Regression in [12] and with Artificial Neural Networks (ANN) in [13, 14]. In this work we apply the Artificial Neural Network Venn Predictor (ANN-VP) to the problem of detecting VUR based on a dataset consisting of children diagnosed with UTI and further examined with VCUG. The data were collected by the Pediatric Clinical Information System of Alexandroupolis University Hospital, Greece. We follow a slightly modified version of the approach proposed in [13], so as to address the class imbalance problem of the particular dataset. In particular we incorporate minority oversampling and majority undersampling in the ANN-VP and compare the performance of the two approaches. Our experimental results show that the probabilistic outputs of the ANN-VPs outperform the ones of conventional ANN in all cases, while minority oversampling performs better than majority undersampling. Furthermore we demonstrate that the probability bounds produced by Venn Prediction are well-calibrated as opposed to the ones produced by conventional ANNs which can be very misleading.

The rest of this paper starts with a review of related work on the prediction of VUR in the next section. This is followed by a description of the dataset used in this study in Section 3. Then in Section 4 it gives overview of the Venn Prediction framework, while in Section 5 it details the proposed ANN-VP with Minority Oversampling and ANN-VP Majority Undersampling algorithms. Section 6 presents the experiments performed in both the batch and on-line settings and reports the obtained results. Finally, Section 7 gives the conclusions and future directions of this work.

2. Related Work

There are some studies in the literature for the prediction of VUR without the use of Artificial Intelligence techniques, which however seem to have very low specificity. The two most recent ones are [7, 16]. In [7] the authors propose a clinical decision rule for predicting VUR of grade III or higher. The rule was derived using a total of 494 patients and it had a sensitivity of 86% and a specificity of 43% in internal cross-validation. In [16] the authors explore the use of Dimercaptosuccinic Acid scan and Ultrasonography for predicting VUR. They report a sensitivity of 81% and a specificity of 53%.

The only study we were able to find other than the ones of the Democritus University of Thrace group on the prediction of VUR using Machine Learning techniques is [3]. In this study the authors identified a urinary proteome pattern for detecting High-grade VUR (grade IV or V) with the use of sup-

Table 1: VUR clinical and laboratorial parameters together with their values

No.	Parameter	Possible values						
1	Sex	Boy	Girl					
2	Age	<1 year	1-5 years	>5 years				
3	Siblings	1	2	3				
4-8	Systsypm	Fever	Vomit/diarrhea		Anorexia	Weight loss	Others	
9	WBC	<4500	4500-10500		>10500			
10	WBC type	n	L	m	E	b		
11	Ht	<37	37-42	>42				
12	Hb	<11.5	11.5-13.5	>13.5				
13	PLT	<170	170-450	>450				
14	ESR	<20	20-40	>40				
15	CRP	+	-					
16	Bacteria	E.coli	Proteus	Kiebsielas	Strep	Stapf	Pseudom	Other
17-22	Sensitiv	Penicillin	Kefalosp2	Kefalosp3	Aminoglyc	Sulfonamides		
23	Ultrasound	Rsize nrm	Rsize abn	Rstract nrm	Rstract abn	Normal	Other	
24	Dursymp	2 days	3 days	4 days	5 days	>5 days		
25	Starttre	2 days	3 days	4 days	5 days			
26-27	Riskfact	Age <1 year		Ttreat				
28	Collect	U-bag	Catheter	Suprapubic				
29-34	Resistan	Penicillin	Kefalosp2	Kefalosp3	Aminoglyc	Sulfonamides		Other

port vector machines (SVM) on data obtained by capillary electrophoresis coupled to mass spectrometry. The resulting proteome test was validated on 36 patients with 88% sensitivity and 79% specificity.

The studies [8, 9, 10] were performed on the same dataset we use here, however only a particular part of it consisting of 20% of the cases was used for testing. In [10] the authors studied the use of multilayer perceptrons, in [9] the authors studied the use of probabilistic neural networks (PNNs) and in [8] the PNNs were combined with a genetic algorithm for optimization of the feature subset and parameters used. The best results were achieved in [8], with a best accuracy of 96.3% on the particular test set. However when tested on the whole dataset in a 10-fold cross-validation setting all PNNs proposed had very low sensitivity.

It's worth to note that none of the approaches proposed in these studies provide any type of probabilistic outputs which is the aim of this work.

3. Vesicoureteral Reflux Disease Data

The VUR data used in this study, were obtained from the Pediatric Clinical Information System of Alexandroupolis University Hospital, Greece. The dataset consists of 162 child patients with UTI, of which 30 were diagnosed with VUR. The clinical and laboratorial parameters considered are the ones

Table 2: Features selected by the three feature selection techniques

Technique	Selected features
CFS	11, 21, 22, 23 and 27
χ^2 /IG	11, 12, 15, 19, 23, 27 and 28

collected according to the medical protocol of the hospital. In total there were 19 parameters, which include

- general information: sex, age and number of siblings
- the clinical presentation (Systsyp)
- blood laboratory testing results: white blood cell count (WBC), WBC type, haematocrit (Ht), haemoglobine (Hb), platelets (PLT), erythrocyte sedimentation rate (ESR) and C-reactive protein (CRP)
- urine cultures: bacteria
- antibiogramme: sensitivity and resistance to antibiotics
- renal / bladder ultrasound results
- duration of the symptoms (Dursymp)
- start of the treatment (Starttre)
- risk factors: whether the child is less than one year old and an assessment of risk by the attending clinicians (Treat)
- method of urine collection (Collect)

A list of these parameters and their values is given in Table 1. It is emphasized that some of the parameters may take more than one values simultaneously. For example the clinical presentation (Systsyp) can be a combination of symptoms. These parameters were transformed to a binary set of sub-parameters, one for each of their possible values indicating existence (1) or not (0) of the particular value. Therefore the clinical presentation was converted to five parameters, the sensitivity and resistance were converted

to six parameters each and the risk factors to two parameters. For this reason these parameters have a range in the first column of Table 1. After this conversion the total number of parameters was 34.

Due to the large number of parameters and the relatively small number of cases, feature selection was applied to the data so as to avoid overfitting. Specifically, three feature selection techniques were used: correlation-based feature subset selection (CFS) [4] in conjunction with best-first search and the chi-squared (χ^2) and information gain (IG) feature evaluation techniques retaining the features with values above zero. The last two returned the same feature subset so the two subsets reported in table 2 were used in our experiments.

4. The Venn Prediction Framework

This section gives a brief description of the Venn prediction framework; for more details the interested reader is referred to [17]. We are given a training set $\{(x_1, y_1), \dots, (x_l, y_l)\}$ of examples, where each $x_i \in \mathbb{R}^d$ is the vector of attributes for example i and $y_i \in \{Y_1, \dots, Y_c\}$ is the classification of that example. We are also given a new unclassified example x_{l+1} and our task is to predict the probability of this new example belonging to each class $Y_j \in \{Y_1, \dots, Y_c\}$ based only on the assumption that all $(x_i, y_i), i = 1, 2, \dots$ are i.i.d.

The Venn Prediction framework assigns each one of the possible classifications $Y_j \in \{Y_1, \dots, Y_c\}$ to x_{l+1} in turn and generates the extended set

$$\{(x_1, y_1), \dots, (x_l, y_l), (x_{l+1}, Y_j)\}. \quad (1)$$

For each resulting set (1) it then divides the examples into a number of categories and calculates the probability of x_{l+1} belonging to each class Y_k as the frequency of Y_k 's in the category that contains it.

To divide each set (1) into categories it uses what is called a *Venn taxonomy*. A Venn taxonomy is a measurable function that assigns a category $\kappa_i^{Y_j}$ to each example z_i in (1); the output of this function should not depend on the order of the examples. Every Venn taxonomy defines a different Venn Predictor. Typically each taxonomy is based on a traditional machine learning algorithm, called the *underlying algorithm* of the VP. The output of this algorithm for each attribute vector $x_i, i = 1, \dots, l + 1$ after being trained either on the whole set (1), or on the set resulting after removing

the pair (x_i, y_i) from (1), is used to assign $\kappa_i^{Y_j}$ to (x_i, y_i) . For example, a Venn taxonomy that can be used with every traditional algorithm assigns the same category to all examples that are given the same classification by the underlying algorithm. The Venn taxonomy used in this work is defined in the next section.

After assigning the category $\kappa_i^{Y_j}$ to each example (x_i, y_i) in the extended set (1), the empirical probability of each classification Y_k among the examples assigned $\kappa_{l+1}^{Y_j}$ will be

$$p^{Y_j}(Y_k) = \frac{\left| \{i = 1, \dots, l+1 \mid \kappa_i^{Y_j} = \kappa_{l+1}^{Y_j} \ \& \ y_i = Y_k\} \right|}{\left| \{i = 1, \dots, l+1 \mid \kappa_i^{Y_j} = \kappa_{l+1}^{Y_j}\} \right|}. \quad (2)$$

This is a probability distribution for the label of x_{l+1} . After assigning all possible labels to x_{l+1} we get a set of probability distributions that compose the multiprobability prediction of the Venn predictor $P_{l+1} = \{p^{Y_j} : Y_j \in \{Y_1, \dots, Y_c\}\}$. As proved in [17] the predictions produced by any Venn predictor are automatically valid multiprobability predictions. This is true regardless of the taxonomy of the Venn predictor. Of course the taxonomy used is still very important as it determines how efficient, or informative, the resulting predictions are. We want the diameter of multiprobability predictions and therefore their uncertainty to be small and we also want predictions to be as close as possible to zero or one.

The maximum and minimum probabilities obtained for each class Y_k define the interval for the probability of the new example belonging to Y_k :

$$\left[\min_{k=1, \dots, c} p^{Y_j}(Y_k), \max_{k=1, \dots, c} p^{Y_j}(Y_k) \right]. \quad (3)$$

If the lower bound of this interval is denoted as $L(Y_k)$ and the upper bound is denoted as $U(Y_k)$, the Venn predictor finds

$$k_{best} = \arg \max_{k=1, \dots, c} \overline{p(Y_k)}, \quad (4)$$

where $\overline{p(Y_k)}$ is the mean of the probabilities obtained for Y_k , and outputs the class $\hat{y} = Y_{k_{best}}$ as its prediction together with the interval $[L(\hat{y}), U(\hat{y})]$ as the probability interval that this prediction is correct. The complementary interval $[1 - U(\hat{y}), 1 - L(\hat{y})]$ gives the probability that \hat{y} is not the true classification of the new example and it is called the *error probability interval*.

In this case however, due to the class imbalance of the data and the much higher prior probability of the negative class, a threshold was used for determining the prediction of our Venn predictors. Specifically, a Venn predictor outputs $\hat{y} = 1$ as its prediction if the mean probability of the positive class $\overline{p(1)}$ is above a given threshold θ and $\hat{y} = 0$ otherwise. The probability interval for the prediction being correct remains $[L(\hat{y}), U(\hat{y})]$.

5. Artificial Neural Networks Venn Prediction with Minority Oversampling or Majority Undersampling

This section describes the Venn Taxonomy used in this work, which is based on ANN, and gives the complete algorithm of the proposed approach. The ANNs used were 2-layer fully connected feed-forward networks with tangent sigmoid hidden units and a single logistic sigmoid output unit. They were trained with the variable learning rate backpropagation algorithm minimizing cross-entropy error. As a result their outputs can be interpreted as probabilities for class 1 and they can be compared with those produced by the Venn predictor. Early stopping was used based on a validation set consisting of 20% of the corresponding training set.

In order to address the class imbalance problem of the data two approaches were examined: minority oversampling (MO) and majority undersampling (MU). Specifically, in the case of the MO approach before training the ANN examples belonging to the minority class were randomly selected with replacement and copied again into the training set until the number of positive and negative examples became equal. In the case of the MU approach a random subset of the majority class examples equal to the size of the minority class was selected to be included in the training set and the remaining majority class examples were not used for training. In both cases this resulted in training the ANN with an equal number of positive and negative examples.

After adding the new example (x_{l+1}, Y_j) to the oversampled or undersampled training set and training the ANN, the output o_i produced by the ANN for each input pattern x_i was used to determine its category κ_i . Specifically the range of the ANN output $[0, 1]$ was split to a number of equally sized regions λ and the same category was assigned to the examples with output falling in the same region. In other words each one of these λ regions defined one category of the taxonomy.

Algorithm 1: ANN-VP with MO/MU

Input: training set $T_o = \{(x_1, y_1), \dots, (x_l, y_l)\}$, test example x_{new} ,
number of categories λ , threshold θ .

Oversample the minority class generating the training set

$T_m = \{(x_1, y_1), \dots, (x_n, y_n)\}$, where $n > l$ OR undersample the
majority class generating the training set

$T_m = \{(x_1, y_1), \dots, (x_n, y_n)\}$, where $n < l$;

for $k = 0$ **to** 1 **do**

Train the ANN on the extended T_m set

$\{(x_1, y_1), \dots, (x_n, y_n), (x_{new}, k)\}$;

Supply the input patterns x_1, \dots, x_l, x_{new} to the trained ANN to
obtain the outputs o_1, \dots, o_l, o_{new} ;

for $i = 1$ **to** l **do**

Assign κ_i to (x_i, y_i) based on the output o_i ;

end

Assign κ_{new} to (x_{new}, k) based on the output o_{new} ;

$$p^k(1) := \frac{|\{i=1, \dots, l, new | \kappa_i^k = \kappa_{new}^k \ \& \ y_i=1\}|}{|\{i=1, \dots, l, new | \kappa_i^k = \kappa_{new}^k\}|},$$

$$p^k(0) := 1 - p^k(1);$$

end

if $\overline{p(1)} > \theta$ **then**

$$\hat{y} = 1$$

else

$$\hat{y} = 0$$

end

Output:

Prediction \hat{y} ;

The probability interval for \hat{y} : $[\min_{k=0,1} p^k(\hat{y}), \max_{k=0,1} p^k(\hat{y})]$.

Using this taxonomy we assigned a category κ_i^0 to each example (x_i, y_i) in the original training set extended with $(x_{l+1}, 0)$ and a category κ_i^1 to each example (x_i, y_i) in the original training set extended with $(x_{l+1}, 1)$. It is important to note that the MO and MU approaches are only part of the taxonomy used and the original (non oversampled or undersampled) training set should be used for calculating the multiprobability predictions with (2). We then followed the process described in Section 4 to calculate the outputs of the ANN Venn Predictor with Minority Oversampling (ANN-VP with MO) and of the ANN Venn Predictor with Majority Undersampling (ANN-VP with MU), which is presented in Algorithm 1.

6. Experimental Results

We performed experiments in both the batch setting and the on-line setting. The former is the standard setting for evaluating machine learning algorithms in which the algorithm is trained on a given training set and its performance is assessed on a set of test cases. In the on-line setting examples are predicted one by one and immediately after prediction their true classification is revealed and they are added to the training set for predicting the next example; the algorithm is re-trained each time on the growing training set. We use this setting to demonstrate the empirical validity of the multiprobability outputs produced by the ANN-VPs.

Before each training session all attributes were normalised setting their mean value to 0 and their standard deviation to 1. For all experiments with conventional ANN, minority oversampling or majority undersampling was performed on the training set in the same way as for the proposed approaches.

6.1. Batch Setting Results

This subsection examines the performance of the proposed approaches with the two feature subsets reported in table 2 in the batch setting and compares their performance to that of the original ANN-VP, to that of the corresponding conventional ANNs and to that of the best approach developed in previous studies on the same data. Specifically we compare it to the third PNN proposed in [8] (we actually tried out all five PNNs of the same study and this was the one that gave the best results). Furthermore, it examines the effect that different choices for the number of taxonomy categories λ have.

For these experiments we followed a 10-fold cross-validation process for 10 times with different divisions of the dataset into the 10 folds and the results reported here are the mean values over all runs. The ANNs used consisted of 5 hidden units, which is a sensible choice for the small number of features selected. The threshold θ used for determining the prediction for all three Venn predictors was set to 0.1852, which is the frequency of the positive examples in the dataset.

In order to be able to use standard metrics for the evaluation of probabilistic outputs, which evaluate single probabilities rather than probability intervals, we convert the output of the ANN-VPs to $\overline{p(1)}$; corresponding to the estimate of the ANN-VP for the probability of each test example being positive. For reporting these results five quality metrics are used. The first two are the sensitivity and specificity of each classifier, which do not take into account the probabilistic outputs produced, but are typical metrics for assessing the quality of classifiers. The third is cross-entropy error (or log-loss):

$$CE = - \sum_{i=1}^N y_i \log(\hat{p}_i) + (1 - y_i) \log(1 - \hat{p}_i), \quad (5)$$

where N is the number of test examples and \hat{p}_i is the probability produced by the algorithm for each test example being positive; this is the error minimized by the training algorithm of the ANNs on the training set. The fourth metric is the Brier score [1]:

$$BS = \frac{1}{N} \sum_{i=1}^N (\hat{p}_i - y_i)^2. \quad (6)$$

The cross-entropy error, or log-loss, and the Brier score are the most popular quality metrics for probability assessments.

The Brier score can be decomposed into three terms interpreted as the uncertainty, reliability and resolution of the probabilities, by dividing the range of probability values into a number of intervals K and representing each interval $k = 1, \dots, K$ by a ‘typical’ probability value r_k [11]. The reliability term of this decomposition measures how close the output probabilities are to the true probabilities and therefore reflects how well-calibrated the output probabilities are. Since the reliability of probabilities is of paramount importance in a medical setting, this is the fifth metric used here. It is defined in

Features	Algorithm	Sens.	Spec.	CE	BS	REL
CFS	ANN-VP	64.33%	84.17%	618.45	0.1165	0.0019
	ANN-VP + MO	75.67%	84.09%	558.92	0.0988	0.0041
	ANN + MO	70.33%	85.83%	697.67	0.1309	0.0350
	ANN-VP + MU	72.33%	79.17%	609.57	0.1130	0.0039
	ANN + MU	61.33%	83.03%	921.19	0.1750	0.0569
χ^2/IG	ANN-VP	67.00%	81.67%	614.39	0.1143	0.0027
	ANN-VP + MO	71.33%	84.70%	595.96	0.1087	0.0052
	ANN + MO	66.00%	86.06%	773.30	0.1411	0.0370
	ANN-VP + MU	66.00%	76.44%	652.33	0.1234	0.0032
	ANN + MU	58.00%	79.17%	897.42	0.1806	0.0576
PNN 3 from [8]		53.00%	92.95%	-	-	-

Table 3: Performance of the two ANN-VPs in the batch setting with the two different feature subsets and comparison with that of the original ANN-VP, of the corresponding conventional ANNs and of the best previously proposed approach.

[11] as:

$$REL = \frac{1}{N} \sum_{k=1}^K n_k (r_k - \phi_k)^2, \quad (7)$$

where n_k is the number of examples with output probability in the interval k and ϕ_k is the percentage of these examples that are positive. Here the number of categories K was set to 20.

Table 3 reports the performance of the two ANN-VPs proposed in this work together with that of the original ANN-VP (without MO or MU, but with the same threshold), of the corresponding conventional ANNs and of the best previously proposed approach for the same data. The first five rows report the results obtained using the features selected with the Correlation-based Feature Selection (CFS) technique, the sixth to the tenth row report the results obtained using the features selected based on the χ^2 and Information Gain (IG) feature evaluation (since both methods selected exactly the same features), the last row reports the results obtained with PNN 3 from [8], which was the best performing approach on the particular data proposed so far. The results of the ANN-VPs reported here were obtained with the number of taxonomy categories λ set to 6, which was the value used in previous studies [13, 15]. However as it is shown in the tables that follow the particu-

Features	λ	Sens.	Spec.	CE	BS	REL
CFS	2	77.00%	84.09%	585.40	0.1097	0.0107
	3	73.33%	84.77%	564.71	0.1025	0.0047
	4	75.33%	84.62%	564.82	0.1010	0.0058
	5	74.67%	84.85%	563.13	0.1005	0.0055
	6	75.67%	84.09%	558.92	0.0988	0.0041
	7	76.00%	84.55%	557.52	0.0987	0.0050
	8	74.00%	84.24%	556.25	0.0979	0.0031
	9	76.00%	83.56%	556.21	0.0984	0.0030
	10	76.33%	84.24%	557.91	0.0991	0.0029
	χ^2/IG	2	73.33%	83.03%	616.83	0.1155
3		71.00%	85.61%	593.93	0.1090	0.0055
4		71.33%	84.39%	606.36	0.1109	0.0066
5		72.00%	84.55%	606.33	0.1111	0.0071
6		71.33%	84.70%	595.96	0.1087	0.0052
7		71.67%	83.79%	599.44	0.1084	0.0046
8		71.67%	83.18%	596.57	0.1080	0.0042
9		71.67%	83.26%	599.08	0.1090	0.0040
10		74.00%	83.48%	601.01	0.1090	0.0057

Table 4: Performance of the ANN-VP with MO in the batch setting with different λ .

lar value does not affect the results by much. It should be noted that for the first two metrics higher values correspond to better performance, whereas for the last three metrics lower values correspond to better performance.

Comparing the sensitivity and specificity values reported in table 3 we see that the proposed ANN-VP with MO had higher sensitivity than the original ANN-VP with both feature subsets. The ANN-VP with MU on the other hand, had higher sensitivity than the original ANN-VP when using the feature subset selected by CFS, but a lower one when using the subset selected by χ^2 and IG. Both proposed ANN-VPs (with MO and MU) always had higher sensitivity than the corresponding conventional ANNs, whereas the opposite happens in the case of specificity. In the case of the previously proposed PNN it seems that its sensitivity is extremely low. However, since in this work we are mainly interested in probabilistic outputs, the main comparison is on the last three metrics. Here the superiority of the VPs is

Features	λ	Sens.	Spec.	CE	BS	REL
CFS	2	73.33%	76.97%	648.90	0.1230	0.0049
	3	66.33%	80.91%	638.80	0.1202	0.0052
	4	73.00%	79.09%	619.42	0.1155	0.0029
	5	72.67%	80.38%	615.46	0.1148	0.0046
	6	72.33%	79.17%	609.57	0.1130	0.0039
	7	75.00%	80.76%	586.90	0.1078	0.0044
	8	74.33%	79.92%	597.02	0.1098	0.0036
	9	75.00%	80.38%	589.38	0.1079	0.0031
	10	75.33%	79.92%	591.32	0.1090	0.0029
	χ^2/IG	2	64.33%	72.65%	696.15	0.1338
3		64.33%	77.65%	668.30	0.1279	0.0028
4		67.67%	77.58%	661.95	0.1258	0.0026
5		65.67%	76.14%	659.12	0.1246	0.0034
6		66.00%	76.44%	652.33	0.1234	0.0032
7		65.67%	76.36%	656.83	0.1234	0.0035
8		67.33%	75.30%	658.08	0.1235	0.0039
9		69.00%	75.91%	659.91	0.1240	0.0034
10		66.33%	75.68%	665.58	0.1246	0.0045

Table 5: Performance of the ANN-VP with MU in the batch setting with different λ .

very clear since in all cases the VPs give lower values than the corresponding conventional ANNs. In fact the difference in reliability is impressive, which shows that even after reducing the probabilistic bounds produced by the two VPs to single probabilities, they are still very reliable.

By comparing the ANN-VP with MO to the ANN-VP with MU and the original ANN-VP approaches we see that the former always performs better at the CE and BS metrics. Reliability is more or less at the same levels for the three methods; the small differences are not really significant for this metric. The majority undersampling approach does not result in a clear improvement as expected. This is most likely due to the small size of the minority class, which makes the training set after majority undersampling very small. It would be interesting to check how its performance is affected when more data are collected. Overall the best performance was obtained with the ANN-VP with MO when using the features selected with the CFS

technique.

Tables 4 and 5 report the performance of the ANN-VP with minority oversampling and the ANN-VP with majority undersampling respectively with different number of categories λ for their taxonomy using the two feature subsets. We can see that the number of categories does not affect the results to a big degree. However the values above 6 or 7 seem to give a somewhat better performance than smaller ones.

6.2. On-line Setting Results

This subsection presents the results obtained when applying the ANN-VP and conventional ANN approaches with minority oversampling in the on-line setting; we examine the minority oversampling approach as it gave the best results in the batch setting. Specifically, in this setting each experiment started with an initial training set of 5 examples and one by one the remaining 157 examples were predicted in turn and immediately after prediction their true classification was revealed and they were added to the training set for predicting the next example. In order to demonstrate that the choice of hidden units and number of taxonomy categories λ does not affect the validity of the resulting probabilistic outputs, we performed this experiment with 5 and 100 hidden units and with λ set to 2, 6 and 10. The results are presented in Figures 1 and 2 in the form of the following three curves for each experiment:

- the cumulative error curve

$$E_n = \sum_{i=1}^n err_i, \quad (8)$$

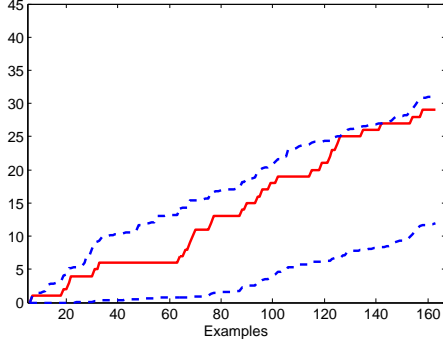
where $err_i = 1$ if the prediction \hat{y}_i is wrong and $err_i = 0$ otherwise,

- the cumulative lower error probability curve

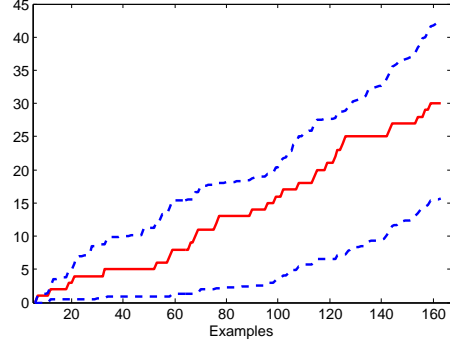
$$LEP_n = \sum_{i=1}^n 1 - U(\hat{y}_i) \quad (9)$$

- and the cumulative upper error probability curve

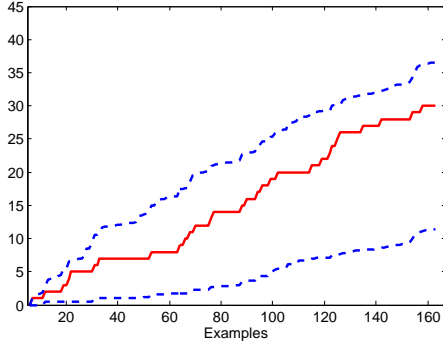
$$UEP_n = \sum_{i=1}^n 1 - L(\hat{y}_i). \quad (10)$$



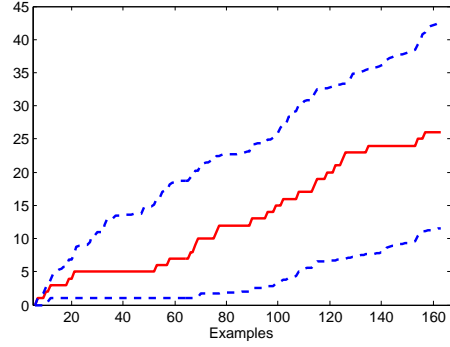
(a) 5 Hidden Units with $\lambda = 2$



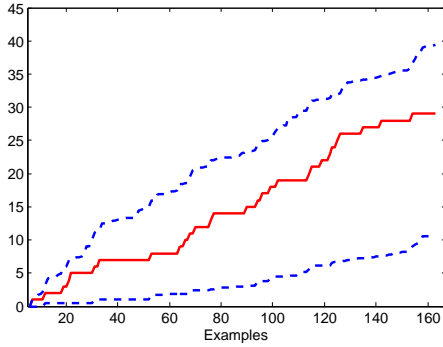
(b) 100 Hidden Units with $\lambda = 2$



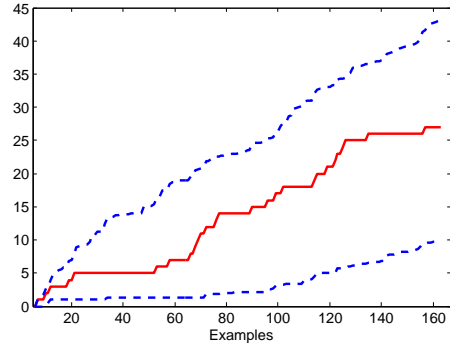
(c) 5 Hidden Units with $\lambda = 6$



(d) 100 Hidden Units with $\lambda = 6$

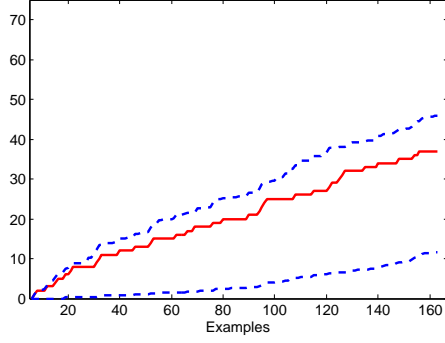


(e) 5 Hidden Units with $\lambda = 10$

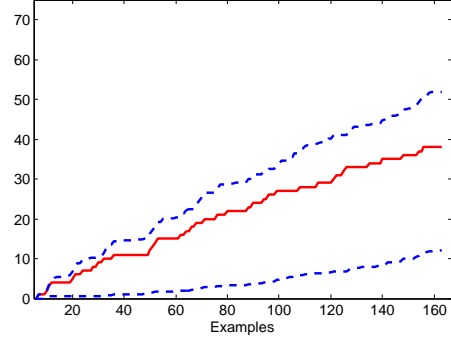


(f) 100 Hidden Units with $\lambda = 10$

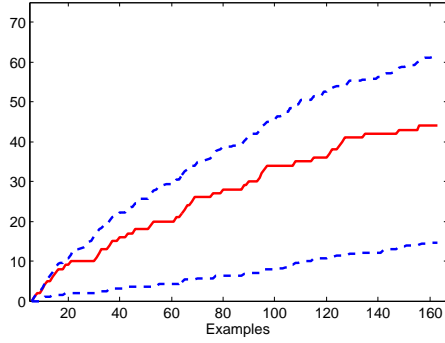
Figure 1: On-line performance of ANN-VP with MO using the feature subset selected by CFS. Each plot shows the cumulative number of errors E_n with a solid line and the cumulative lower and upper error probability curves LEP_n and UEP_n with dashed lines.



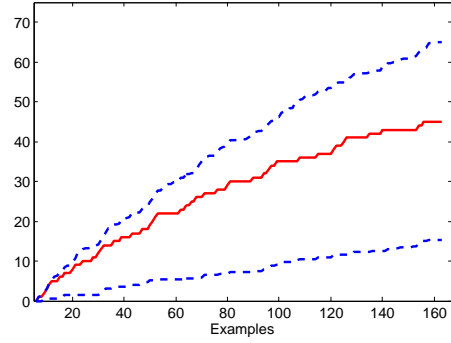
(a) 5 Hidden Units with $\lambda = 2$



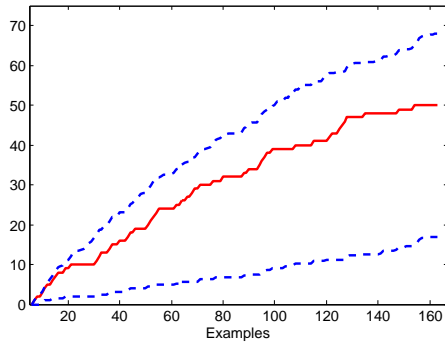
(b) 100 Hidden Units with $\lambda = 2$



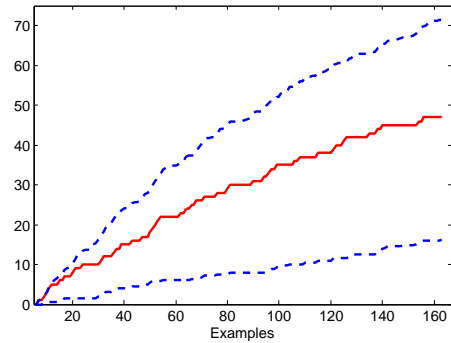
(c) 5 Hidden Units with $\lambda = 6$



(d) 100 Hidden Units with $\lambda = 6$

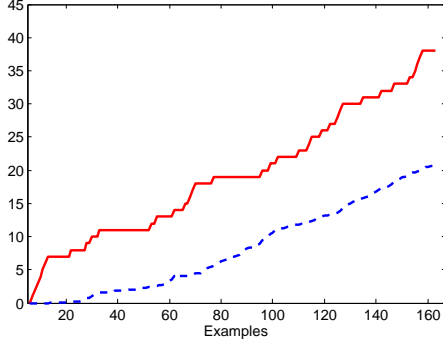


(e) 5 Hidden Units with $\lambda = 10$

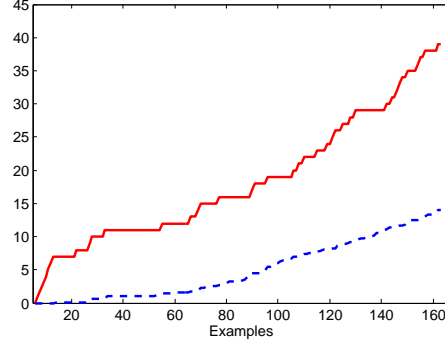


(f) 100 Hidden Units with $\lambda = 10$

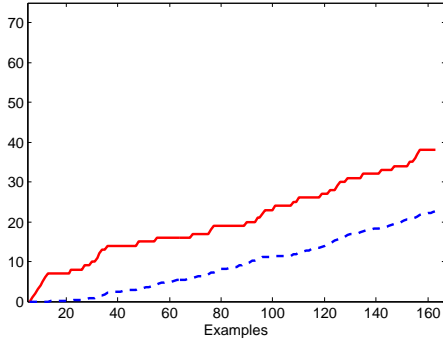
Figure 2: On-line performance of ANN-VP with MO using the feature subset selected by χ^2 and IG. Each plot shows the cumulative number of errors E_n with a solid line and the cumulative lower and upper error probability curves LEP_n and UEP_n with dashed lines.



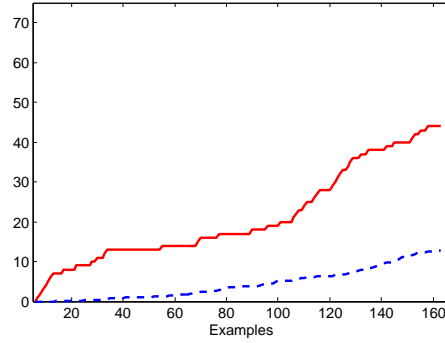
(a) 10 Hidden Units - CFS features



(b) 100 Hidden Units - CFS features



(c) 10 Hidden Units - χ^2 /IG features



(d) 100 Hidden Units - χ^2 /IG features

Figure 3: On-line performance of the original ANN with MO classifier. Each plot shows the cumulative number of errors E_n with a solid line and the cumulative error probability curve EP_n with a dashed line.

The plots on the left present the results with 5 hidden units while the plots on the right present the results with 100 hidden units. In terms of the number of taxonomy categories the top plots present the results with 2 categories, the middle plots present the results with 6 categories and the bottom plots present the results with 10 categories. The plots confirm that the probability intervals produced by ANN-VP are well-calibrated since the cumulative errors are always included inside the cumulative upper and lower error probability curves. This shows that the ANN-VP will produce well-calibrated upper and lower error probability bounds regardless of the choice of features and taxonomy parameters. Note that although the use of the feature sub-

set selected by χ^2 and IG (figure 2) gives a higher number of errors than the one generated with CFS (figure 1), the bounds of the VP remain well-calibrated, they just become wider to accommodate the higher uncertainty. Also the bounds generated with 100 hidden units are again wider than those generated with 5. Finally it seems that increasing the number of taxonomy categories also gives wider probability bounds possibly due to the relatively small size of the dataset.

The same experiment was performed with the original ANN classifier (with MO) on the two feature subsets and analogous plots are displayed in Figure 3. The two top plots present the results when using the feature subset selected by CFS while the two bottom plots present the results when using the feature subset selected by χ^2 and IG. In this case the cumulative error curve (8) is plotted together with the cumulative error probability curve

$$EP_n = \sum_{i=1}^n |\hat{y}_i - \hat{p}_i|, \quad (11)$$

where $\hat{y}_i \in \{0, 1\}$ is the ANN prediction for example i and \hat{p}_i is the probability given by ANN for example i belonging to class 1. In effect this curve is a sum of the probabilities of the less likely class for each example according to the ANN. One would expect that this curve would be near the cumulative error curve if the probabilities produced by the ANN were well-calibrated. The plots of Figure 3 show that this is not the case. The ANNs underestimate the true error probability in both cases since the cumulative error curve is much higher than the cumulative error probability curve. To check how misleading the probabilities produced by the ANN are, the 2-sided p -value of obtaining the resulting total number of errors E_N with the observed deviation from the expected errors EP_N given the probabilities produced by the ANN was calculated for each case. The resulting p -values for the ANNs with 5 hidden units were 0.000019458 with the CFS feature subset and 0.0001704 with the χ^2 /IG feature subset. The corresponding p -values for the ANNs with 100 hidden units were even smaller; actually much smaller. This shows how misleading the probabilities produced by conventional ANNs can be, as opposed to the well-calibrated bounds produced by VPs.

7. Conclusions

This study applied Venn Prediction coupled with ANNs to the problem of VUR detection. In order to address the class imbalance problem of the

particular task, minority oversampling and majority undersampling were incorporated in the ANN Venn Predictor. Unlike conventional classifiers the proposed approach produces lower and upper bounds for the conditional probability of each child having VUR, which are valid under the general i.i.d. assumption.

Our experimental results show the superiority of the VP approaches over conventional ANNs. The difference is especially significant in the case of the reliability metric, which points out that conventional ANNs can be quite unreliable as opposed to the proposed approaches. The proposed ANN-VP with MO outperforms all other methods while its comparison with the original ANN-VP approach shows that majority oversampling results in a big improvement especially in terms of sensitivity.

Moreover our experimental results in the on-line setting demonstrate that the probability bounds produced by ANN-VP with MO are well-calibrated regardless of the feature subset used, number of taxonomy categories and number of hidden units used in the underlying ANN. On the contrary, the single probabilities produced by conventional ANN were shown to be very misleading.

Based on these results we believe that the proposed approach can be used in clinical practice for supporting the decision of whether a child should undergo further testing with VCUG or not. The use of this approach does not require any specialized tests other than the ones already being performed, therefore it can be easily incorporated into clinical practice without any significant costs. But most importantly the guaranteed reliability of the probabilistic bounds it produces means that they can be used by clinicians for taking informed decisions without the risk of being misled as cases with high uncertainty will be indicated either by very wide probabilistic bounds or by probabilities near 0.5. Therefore in cases with probabilistic bounds near 0 (negative for VUR) the decision that a VCUG is not needed can be taken with rather high certainty.

The main directions for future work include the assessment of the proposed approach in clinical practice and the collection of a bigger dataset, which will allow drawing more definite conclusions. Finally, experimentation with VPs based on other conventional classifiers is also in our future plans.

References

- [1] G. W. Brier, Verification of forecasts expressed in terms of probability, *Monthly Weather Review* 78 (1) (1950) 1–3.
- [2] M. Dashevskiy, Z. Luo, Reliable probabilistic classification and its application to internet traffic, in: *Proceedings of the 4th international conference on Intelligent Computing (ICIC 2008): Advanced Intelligent Computing Theories and Applications. With Aspects of Theoretical and Methodological Issues*, vol. 5226 of LNCS, Springer, 2008, pp. 380–388.
- [3] J. Drube, E. Schiffer, E. Lau, C. Petersen, M. Kirschstein, M. J. Kemper, R. Lichtinghagen, B. Ure, H. Mischak, L. Pape, J. H. Ehrich, Urinary proteome analysis to exclude severe vesicoureteral reflux, *Pediatrics* 129 (2) (2012) e356–e363.
- [4] M. A. Hall, Correlation-based feature subset selection for machine learning, Ph.D. thesis, University of Waikato, Hamilton, New Zealand (1998).
- [5] H. Holst, M. Ohlsson, C. Peterson, L. Edenbrandt, Intelligent computer reporting ‘lack of experience’: a confidence measure for decision support systems, *Clinical Physiology* 18 (2) (1998) 139–147.
- [6] A. Lambrou, H. Papadopoulos, I. Nouretdinov, A. Gammerman, Reliable probability estimates based on support vector machines for large multiclass datasets, in: *Artificial Intelligence Applications and Innovations (AIAI 2012)*, vol. 382 of IFIP AICT, Springer, 2012, pp. 182–191.
- [7] S. Leroy, C. Romanello, V. Smolkin, A. Galetto-Lacour, B. Korczowski, D. Tuerlinckx, C. Rodrigo, V. Gajdos, F. Moulin, P. Pecile, R. Halevy, A. Gervaix, B. Duhl, T. V. Borght, C. Prat, L. Foix-l’Helias, D. G. Altman, D. Gendrel, G. Breart, M. Chalumeau, Prediction of moderate and high grade vesicoureteral reflux after a first febrile urinary tract infection in children: Construction and internal validation of a clinical decision rule, *The Journal of Urology* 187 (1) (2012) 265–271.
- [8] D. Mantzaris, G. Anastassopoulos, A. Adamopoulos, Genetic algorithm pruning of probabilistic neural networks in medical disease estimation, *Neural Networks* 24 (8) (2011) 842–851.

- [9] D. Mantzaris, G. Anastassopoulos, L. Iliadis, A. Tsalkidis, A. Adamopoulos, A probabilistic neural network for assessment of the vesicoureteral reflux's diagnostic factors validity, in: Proceedings of the 20th International Conference on Artificial Neural Networks (ICANN 2010), vol. 6352 of LNCS, Springer, 2010, pp. 32–41.
- [10] D. Mantzaris, G. Anastassopoulos, A. Tsalkidis, A. Adamopoulos, Intelligent prediction of vesicoureteral reflux disease, WSEAS Transactions on Systems 4 (9) (2005) 1440–1449.
- [11] A. H. Murphy, A new vector partition of the probability score, Journal of Applied Meteorology 12 (4) (1973) 595–600.
- [12] I. Nouretdinov, D. Devetyarov, B. Burford, S. Camuzeaux, A. Gentry-Maharaj, A. Tiss, C. Smith, Z. Luo, A. Chervonenkis, R. Hallett, V. Vovk, M. Waterfield, R. Cramer, J. F. Timms, I. Jacobs, U. Menon, A. Gammerman, Multiprobabilistic venn predictors with logistic regression, in: Artificial Intelligence Applications and Innovations (AIAI 2012), vol. 382 of IFIP AICT, Springer, 2012, pp. 224–233.
- [13] H. Papadopoulos, Reliable probabilistic prediction for medical decision support, in: Proceedings of the 7th IFIP International Conference on Artificial Intelligence Applications and Innovations (AIAI 2011), vol. 364 of IFIP AICT, Springer, 2011, pp. 265–274.
- [14] H. Papadopoulos, Reliable probabilistic classification with neural networks, Neurocomputing 107 (2013) 59–68.
- [15] H. Papadopoulos, G. Anastassopoulos, Probabilistic prediction for the detection of vesicoureteral reflux, in: Proceedings of the 14th International Conference on Engineering Applications of Neural Networks (EANN 2013), vol. 383 of CCIS, Springer, 2013, pp. 253–262.
- [16] H. Sorkhi, H.-G. Nooreddini, M. Amiri, S. Osia, S. Farhadi-Niakee, Prediction of vesicoureteral reflux in children with first urinary tract infection by dimercaptosuccinic acid and ultrasonography, Iranian Journal of Pediatrics 22 (1) (2012) 57–62.
- [17] V. Vovk, A. Gammerman, G. Shafer, Algorithmic Learning in a Random World, Springer, New York, 2005.

- [18] V. Vovk, G. Shafer, I. Nouretdinov, Self-calibrating probability forecasting, in: *Advances in Neural Information Processing Systems 16*, MIT Press, 2004, pp. 1133–1140.
- [19] C. Zhou, I. Nouretdinov, Z. Luo, D. Adamskiy, L. Randell, N. Coldham, A. Gammerman, A comparison of venn machine with platt’s method in probabilistic outputs, in: *Proceedings of the 7th IFIP International Conference on Artificial Intelligence Applications and Innovations (AIAI 2011)*, vol. 364 of IFIP AICT, Springer, 2011, pp. 483–490.